Original Article

The correlation between magnetic resonance diffusion parameters and Ki-67 and PCNA in hepatic fibrosis and cirrhosis rats

Peng Kong, Tianwen Yuan, Yang He, Saibo Wang, Xing Zhou, Jun Cao

Dahua Hospital, Shanghai, China

Contributions: (I) Conception and design: P Kong; (II) Administrative support: J Cao; (III) Provision of study materials or patients: P Kong, T Yuan, Y He; (IV) Collection and assembly of data: P Kong, Y He, X Zhou; (V) Data analysis and interpretation: S Wang; (VI) Manuscript writing: All authors; (VII) Final approval of manuscript: All authors.

Correspondence to: Jun Cao, MD. Dahua Hospital, Xuhui District, Shanghai 200237, China. Email: juncao@sina.com; Caojun90000@hotmail.com.

Background: The aim of this study was to assess the value of different 1.5 T MRI apparent diffusion coefficient (ADC) and exponential apparent diffusion coefficient (EADC) values in diagnosing the stages of liver cirrhosis. Sprague-Dawley (SD) rats were randomly divided into the experimental group and the control group.

Methods: The experimental group was injected with thioacetamide intraperitoneally 3 times per week. After routine MR scanning, diffusion-weighted imaging (DWI) was processed by spin echo-echo planar imaging (SE-EPI) to generate the ADC value and EADC image. The liver ADC and EADC values of rats were measured in the control and experimental groups, followed by Masson staining and hematoxylin and eosin staining. Furthermore, immunohistochemistry was performed to detect Ki-67 and PCNA expression in liver tissues.

Results: In the control group, the differences in ADC and EADC values between the liver fibrosis and cirrhosis group were different. The ADC values of the liver fibrosis stage I–II, III–IV, and cirrhosis rats in the experimental group were lower than the control group, while the EADC values were higher than the control group. The ADC values of the liver fibrosis stage III–IV group and cirrhosis nodules group were lower than the control group. There were significant differences in EADC values between the cirrhotic nodule groups and the control group.

Conclusions: DWI-ADC values showed a negative correlation between SD rat liver fibrosis and cirrhosis pathology classification.

Keywords: Diffusion-weighted imaging (DWI); hepatic fibrosis; hepatic cirrhosis; apparent diffusion coefficient (ADC); exponential apparent diffusion coefficient (EADC)

Submitted Jun 02, 2021. Accepted for publication Jul 22, 2021.

doi: 10.21037/apm-21-1745

View this article at: https://dx.doi.org/10.21037/apm-21-1745

Introduction

The creation of hepatic fibrosis and cirrhosis models has contributed to research using magnetic resonance imaging (MRI). MRI diffusion-weighted imaging (DWI) is an imaging technology which can reflect the free diffusion of water molecules, and its apparent diffusion coefficient (ADC) and exponential apparent diffusion coefficient (EADC) parameters have preferable clinical application value. Moreover, the expression levels of Ki-67 and proliferating cell nuclear antigen (PCNA) have high value for diagnosing the stages of liver cirrhosis. This study investigated the role and relevance of the ADC and EADC, and the expression of Ki-67 and PCNA in the process of hepatic fibrosis. Furthermore, MR-DWI can reflect the pathological progression from liver fibrosis to liver cirrhosis at the molecular level, and is a noninvasive imaging method for research on hepatic fibrosis (1-3). By measuring the quantitative changes in ADC and

EADC values, histopathological variations in the progression from liver fibrosis to liver cirrhosis can be objectively and integrally exhibited, and repetitive examinations are also available using this method which is ideal for diagnosing liver fibrosis and liver cirrhosis on imaging. PCNA and Ki-67 are mature markers that indicate cell proliferation, and in recent years they have been mainly utilized in various kinds of cancer research (4,5). High expression of PCNA reveals abundant synthesis of DNA in cells, which makes PCNA an excellent biomarker in the synthesis phase. As a PCNA, Ki-67 is expressed in the cell cycle except G0, and the most prominent expression can be seen in G2 and M. It should be noted that *in vitro* studies may show different results from *in vivo* findings related to liver fibrosis. In this study, we revealed the association between the value of the correlation between MR diffusion parameters and Ki-67 or PCNA, and this finding will provide information for clinical diagnosis and treatment strategies. We present the following article in accordance with the ARRIVE reporting checklist (available at https://dx.doi.org/10.21037/apm-21-1745).

Methods

Experimental animals

Sprague-Dawley (SD) rats (male, aged 6–7 weeks) weighing 180–200 g were used in the study. SD rats were purchased from Shanghai Rui Tai Mo Si Biotechnology, and maintained by the Experimental Animal's Center of Shanghai Vocational College of Agriculture and Forestry according to standard methods. This study was approved by the Ethics Committee of Dahua Hospital of Xuhui District, in compliance with Dahua Hospital of Xuhui District guidelines for the care and use of animals.

Experimental procedures

SD rats (n=100) were randomly assigned into 2 groups: the experimental group (n=84) and the control group (n=16). The animal model was made according to procedure described by Tripathi DM (6). Briefly, the experimental group was treated with thioacetamide (TAA) intraperitoneal injection (i.p.) which was used to induce liver fibrosis and cirrhosis, and TAA (200 mg/kg, i.p.) was used 3 times a week until the 30th week. Meanwhile, rats in the control group were treated with normal saline (NS) at the same dose 3 times a week. Totally, 70% successful rate of animal model was achieved (control group: 12/16, experimental group: 57/84).

Gross observations

During the process of inducing hepatic fibrosis and hepatic cirrhosis, rats in the experimental group were observed in terms of activity and irritation, and details and time of death were recorded. In the 6th week, to obtain liver samples, the first batch of rats were sacrificed under deep anesthesia. Subsequently, these rats were sacrificed to harvest livers until the 30th week, and 1–5 rats were sacrificed every week to dynamically investigate changes in liver morphology and organization. Histological sections were obtained to further observe these livers. Meanwhile, 1 or 2 rats in the control group were sacrificed at the same time when experimental rats were sacrificed.

MRI examinations

A 1.5 T superconductive MRI system (Philips, Holland) with a special coil for small animals (inner diameter 3 inches, orthogonal coil) was utilized to observe rats anesthetized by 10% chloral hydrate (2 mg/kg). Rats were covered with gauze and placed in the center of the coil. After scanning of the conventional transverse axis, coronal T_2WI and T_1WI fast spin echo-echo planar imaging (FSE-EPI) was used to perform DWI in hepatoscopy with fixed parameters such as TR 840 ms, TE 57 ms, number of signal averages (NSA) 10, matrix 68×128, and the values of b were 0 s/mm^2, 300 s/mm^2, and 600 s/mm^2. Sensitive gradient pulses were applied in the X, Y, and Z axis, and the scans lasted for 2 min and 42 s. Except for artifacts caused by breathing, abdominal movement, and death during the examinations, 69 rat liver images were obtained. Two regions of interest (ROIs) were selected randomly in every rat left lobe and right lobe separately to measure the ADC and EADC values. The areas of ROIs were 5–10 mm^2. Every sample was scanned in 3 layers producing 6 results. Liver nodules (diameter >5 mm) were directly measured for the ADC and EADC, and ROIs were calculated as averages. In this study, when b=300 s/mm^2, the liver fibrosis was diagnosed as stage I–II, III–IV group and cirrhosis of the liver nodules group of ADC value. While b=600 s/mm^2 group, ADC value of liver fibrosis stage III–IV group.

Histopathological examination

At 24 h after the MRI, livers with thicknesses of

Table 1 Characters of cirrhotic nodules of each stage under microscopy (*Figure 1*)

Stage	Characters
I	Fibrosis around the central vein, circumferential and intralobular fibrosis
II	Fibrosis limited around the central vein, with preserved hepatic lobular structure
III	Bridging fibrosis dissecting the lobular structure, representing cirrhosis of the liver
IV	Cirrhosis of the liver, with diffuse proliferation of fibrous tissue in multiple parts of the entire lobule, and more extensive fibrosis with formation of pseudolobules

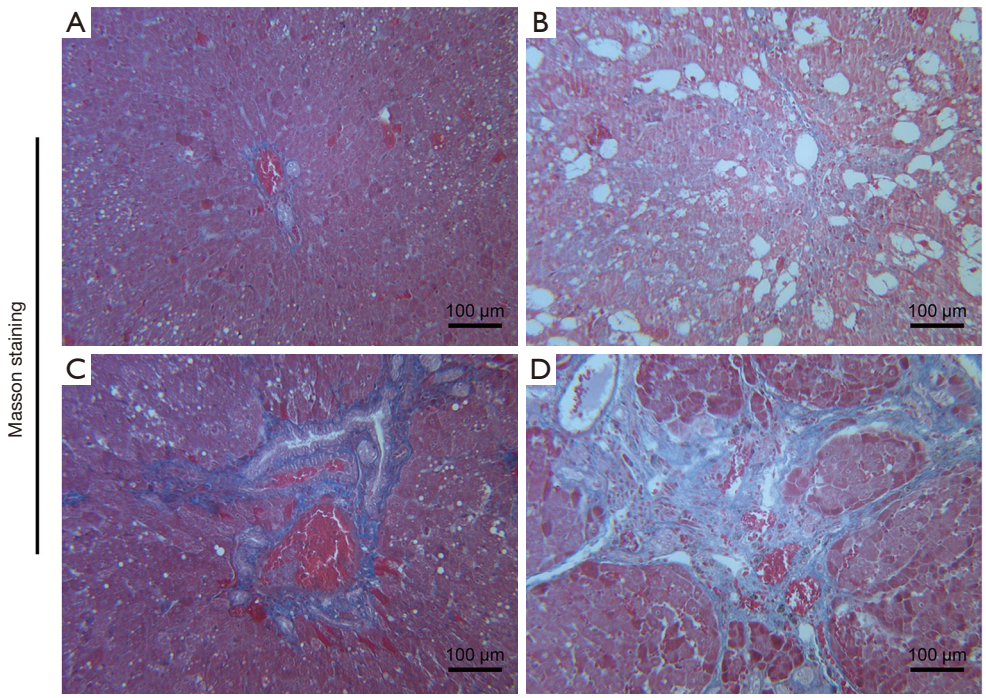

Figure 1 The liver fibrosis staging criteria used in this study. (A) Level I, collect abbacy fibrosis, within limited fibrosis. (B) Level II, portal area around fibrosis, fiber interval to form, lobular structures remain. (C) Level III, fiber structure makes the lobule structure disorder, cirrhosis of the liver. (D) Level IV, early cirrhosis, fibrous tissue in the lobule is more diffuse hyperplasia, false flocculus to form, and there are 3 level also changed. Magnification ×200.

approximately 3–4 mm were harvested along the MRI transverse section. After being fixed by 10% neutral-buffered formalin, these samples were used to make paraffin sections, followed by hematoxylin and eosin (HE) staining and Masson staining. Two pathologists microscopically observed the liver area, including fibrosis around the central vein and hyperplasia. These results were divided into stages 0-IV of liver fibrosis by 2 pathologists according to the liver fibrosis staging criteria (7). Meanwhile, the stages of cirrhotic nodules were determined by microscopy (*Table 1*, *Figure 1*).

Immunohistochemistry

PCNA and Ki-67 staining was performed according to the immunohistochemical protocol. Liver tissues were used as positive controls for PCNA and Ki-67, and PBS was utilized as a negative control instead of primary antibodies. Five suitable views were selected under magnification of 400× in each section and 200 cells were counted in every view. Each section was observed by microscope and recorded the field to evaluate the score of positive cell proportion and color shades and semi-quantitative analysis. Positive cell staining judgment (A): 0 marks for less than 5%, 1 mark for 5–25%,

2 marks for 26–50%, 3 marks for 5–75%, and 4 marks for higher than 75%. Determination of positive intensity (B): 0 points for light yellow without coloring or consistent with the background, 1 point for light brown yellow, 2 points for brown yellow, and 3 points for tan. Results were determined according to 2 indicators of the number of points (integral number = A * B). In this study, mouse monoclonal antibody PCNA (Hangzhou Lianke Biology Co., LTD, 61-959551) and mouse polyclonal antibody (Boster, A00254) were used, along with. Immunohistochemical secondary antibody: SA1021-mouse. The immunohistochemical DAB color development kit (Bausch, Wuhan) and Masson staining kit (Bausch, Wuhan) were also used.

In terms of the number of samples for histopathological assessment, 16 were pathologically diagnosed as stage 0 hepatic fibrosis (12 were successful on DWI); 18 were diagnosed as liver fibrosis stage I–II, 30 were diagnosed as liver fibrosis stage III–IV, cirrhosis of the liver nodules period only 21.

Statistical analysis

All data were presented as mean ± standard deviation (SD). An unpaired Student's *t*-test was used for comparisons between 2 groups. A one-way analysis of variance (ANOVA) followed by Bonferroni post hoc test was used for comparisons among multiple groups as appropriate. A two-sided $P<0.05$ was considered statistically significant. The values of ADC and EADC from different b values were evaluated by correlation with the pathology type by Spearman analysis. Statistical analysis was performed with SPSS 20.

Results

Animal observations and pathological classifications

Survival rates and success rates

In the control group, 16 rats remained alive and 12 of them were successful samples for the investigation. As for the experimental group, after the MRI examination there were 15 dead rats and the mortality rate was 18% (15/84), and 57 of the alive rats were successful samples for the investigation.

Degree of liver damage

The grading standards for the degree of liver fibrosis were as follows: stage 0, no fibrosis; stage 1, fibrotic enlargement of the portal area; stage 2, fibrosis around the portal area, forming a fibrous septum; stage 3, fibrous structure caused lobular structure disorder, without cirrhosis; stage 4, early cirrhosis.

Rat livers observed in the control group were silky with a uniform dark red color. After the model was established, gradually the rat livers exhibited traumatic hepatitis, hepatic fibrosis, and cirrhosis. At the 6th week to 11th week after modeling, there was hepatic fibrosis in the rat livers. After the 15th week to the 20th week, there were abundant pseudolobules and dysplastic nodules including regenerative nodules and dysplastic nodules which showed diffuse distribution and different sizes. According to the results of the pathological diagnosis, there were 16 rats with stage 0 hepatic fibrosis (12 of them successfully finished DWI examination), 18 rats with stage I–II (15 of them successfully finished DWI examination), 30 rats with stage III–IV (24 of them successfully finished DWI examination), and 21 rats in the stage of cirrhotic nodules (18 of them successfully finished DWI examination).

Results of MRI examinations

Cirrhotic nodules exhibited superior signals on T_1WI and equal or slightly lower signals on T_2WI

Dynamic enhanced T_1WI showed synchronized reinforcement in liver nodules and liver parenchyma, as shown in *Figure 2A,B,C,D,E*. Results of ADC and EADC values increased gradually over time, as shown in *Figure 2F,G*.

T_1WI and T_2WI in rat livers

As for the experimental group, there were no significant changes in morphology and signals of stage I–II hepatic fibrosis. At stage III–IV of hepatic fibrosis, signals were non-homogeneous. At the stage of cirrhotic nodules, contours of rat livers were irregular and the jecoral edge had nodular protrusions. At the same time, some nodules exhibited equal or slightly lower signals on T_1WI and equal or slightly higher signals on T_2WI.

DWI results of rat livers

There were 69 DWI images that were good quality, and 57 of them were from the experimental group while the others were from the control group. Increasing signals in the liver were shown by DWI over time, and images with high b values had more conspicuous signals but poorer image quality. Large cirrhosis had equal or slightly higher signals on DWI, and apparent nodules could be found at the edge

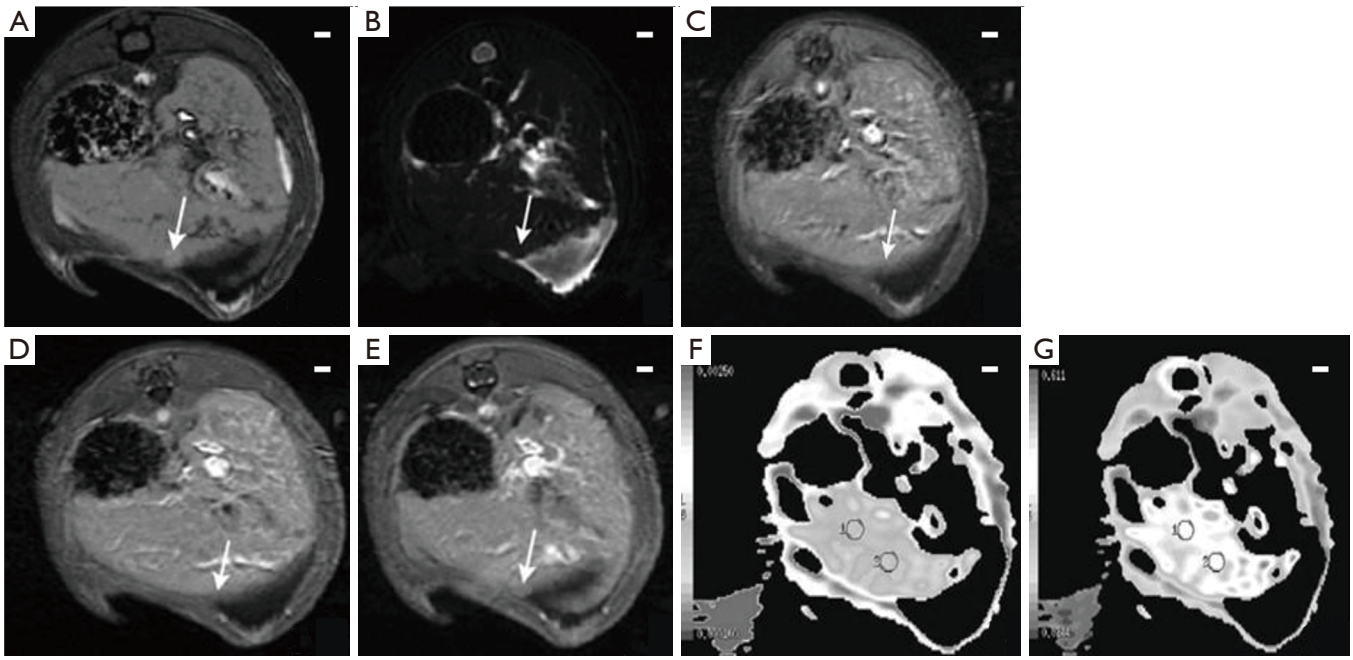

Figure 2 MR imaging of dysplastic nodules in the right hepatic lobes of rats. FSPGR T_1WI exhibited higher signals in the jecoral right lobe nodule with a distinct boundary. (A) FSE and T_2WI which were inhibited by fat revealed inferior signal in the nodule. (B) Dynamic expander in the arterial phase of T_1WI (C) and the venous phase. (D) The display of the liver nodule and liver parenchyma was enhanced synchronously, and lower signal was observed in the delay period. (E) Figures on DWI and ADC (F) and the EADC figure. (G) Display of nodules (at arrow). Scale bar: 1 cm. FSPGR, fast spoiled gradient-echo; FSE, Fast Spin Echo; EADC, exponential apparent diffusion coefficient; DWI, diffusion-weighted imaging; ADC, apparent diffusion coefficient.

of the liver. After selecting ROIs of high quality, ADC and EADC with different b values were measured. As shown in *Tables 2* and *3*, there were certain differences in ADC and EADC values during various stages of hepatic fibrosis and cirrhosis.

The expression of Ki-67 and PCNA in the progression of hepatic fibrosis to cirrhosis

Ki-67 and PCNA have positive cell particles in the normal mouse liver. As for the experimental group, increased positive particles and deepened staining were observed, especially in the later stages of hepatic fibrosis, which had statistical significance compared with the control group, as shown in *Table 4* and *Figure 3*.

The relevance between the values of ADC and EADC and different b values and the expression of Ki-67 and PCNA

When b was fixed at 300 s/mm^2, there was a positive correlation between the ADC value and the expression of Ki-67 and PCNA, and a negative correlation with EADC. The trend of b at 600 s/mm^2 was similar to that of b at 300 s/mm^2 (*Table 5*).

Pathological changes in the progression of hepatic fibrosis to cirrhosis

In *Figure 4*, we observed that the surface of cells in stage I was glossy, and HE showed that vacuoles and inflammatory cell infiltration were obvious (*Figure 4A*). In stage II, the surface of liver tissue was rough, and HE staining showed that the vacuoles in the tissues were significantly increased, along with cell matrix deposition (*Figure 4B*). The surface of liver tissue in stage IV lost its luster and showed a state of sclerosis. HE staining showed inter tissue fibrosis (*Figure 4C*), while in stage VI liver tissue, this fibrosis was further aggravated (*Figure 4D*).

Discussion

MR-DWI can reflect the pathological progression from

Table 2 DWI values when b=300 s/mm^2

Group/parameter	Control group	Experimental group	*t* value	P value
Control group *vs.* stage I–II of hepatic fibrosis				
ADC value	1.38±0.42	1.08±0.49	2.21	0.15
EADC value	0.68±0.08	0.71±0.09	1.70	0.202
Control group *vs.* stage III–IV of hepatic fibrosis				
ADC value	1.38±0.42	0.99±0.49	2.42	0.019
EADC value	0.68±0.08	0.75±0.09	3.65	0.000
Control group *vs.* stage of cirrhotic nodules				
ADC value	1.38±0.42	0.65±0.31	2.80	0.023
EADC value	0.68±0.08	0.82±0.06	3.67	0.000

DWI, diffusion-weighted imaging; ADC, apparent diffusion coefficient; EADC, exponential apparent diffusion coefficient.

Table 3 DWI values when b=600 s/mm^2

Group/parameter	Control group	Experimental group	*t* value	P value
Control group *vs.* stage I–II of hepatic fibrosis				
ADC value	1.05±0.41	0.90±0.40	2.19	0.008
EADC value	0.60±0.13	0.59±0.13	2.65	0.011
Control group *vs.* stage III–IV of hepatic fibrosis				
ADC value	1.05±0.41	0.80±0.35	2.38	0.014
EADC value	0.60±0.13	0.63±0.11	2.68	0.019
Control group *vs.* stage of cirrhotic nodules				
ADC value	1.05±0.41	0.55±0.23	2.40	0.018
EADC value	0.60±0.13	0.76±0.12	2.80	0.023

DWI, diffusion-weighted imaging; ADC, apparent diffusion coefficient; EADC, exponential apparent diffusion coefficient.

Table 4 Ki-67 and PCNA expression

Group/parameter	Control group	Experimental group	*t* value	P value
Control group *vs.* stage I–II of hepatic fibrosis				
Ki-67	1.63±0.36	1.97±0.53	6.34	0.000
PCNA	1.24±0.21	2.31±0.37	4.05	0.000
Control group *vs.* stage III–IV of hepatic fibrosis				
Ki-67	1.63±0.36	3.36±0.65	7.36	0.000
PCNA	1.24±0.21	3.69±0.48	4.28	0.000
Control group *vs.* stage of cirrhotic nodules				
Ki-67	1.63±0.36	4.13±0.84	8.19	0.000
PCNA	1.24±0.21	4.49±0.61	4.13	0.000

DWI, diffusion-weighted imaging; ADC, apparent diffusion coefficient; EADC, exponential apparent diffusion coefficient.

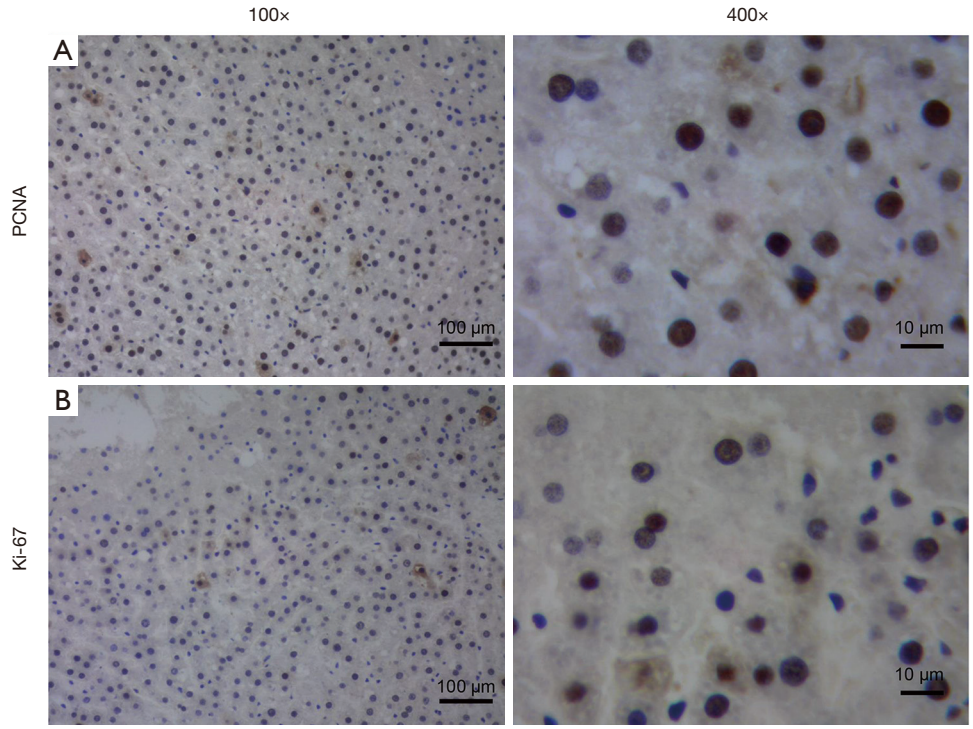

Figure 3 Immunohistochemistry results of rat liver tissues. (A) Rat regenerated nodular liver cells present positive expression of PCNA. (B) Rat hepatocytes with regenerated nodules show Ki-67 expression in liver tissue. PCNA, proliferating cell nuclear antigen.

Table 5 Correlation of Ki-67 and PCNA expression with DWI

Group/parameter	Ki-67	PCNA
b=300 s/mm^2		
ADC value	0.459	0.652
EADC value	−0.739	−0.646
b=600 s/mm^2		
ADC value	0.823	0.731
EADC value	−0.627	−0.648

PCNA, proliferating cell nuclear antigen; DWI, diffusion-weighted imaging; ADC, apparent diffusion coefficient; EADC, exponential apparent diffusion coefficient.

liver fibrosis to liver cirrhosis at the molecular level, and is a noninvasive imaging method for research on hepatic fibrosis (1-3). By measuring the quantitative changes in ADC and EADC values, histopathological variations in the progression from liver fibrosis to liver cirrhosis can be objectively and integrally exhibited, and repetitive examinations are also available with this method, making it an ideal approach for diagnosing liver fibrosis and liver cirrhosis on imaging. Pathological changes such as pseudolobules and intervals between hepatic fibrosis were observed by microscopy.

DWI mainly reflects the movement of water molecules in tissues, represented by the ADC. The EADC image is more convenient to locate and can more accurately measure the degree of water molecule dispersion limitation. The signal contrast is higher than the ADC image, and the lesion edge is clearly displayed, which is consistent with the DWI image.

Ki-67 expression can reflect the proliferation and invasion ability of tumor cells, and is related to the differentiation of hepatocellular carcinoma, which is an important indicator of tumor prognosis. As the degree of chronic hepatitis and liver carcinoma worsened, the Ki-67 index increased. PCNA is synthesized in the nucleus, and changes in its content and expression intensity are consistent with the degree of DNA synthesis and DNA replication. Therefore, PCNA is an indicator of liver regeneration and a useful prognostic indicator. In this study, with the development of liver fibrosis, the value of ADC gradually decreased. A significant negative correlation between these 2 factors was observed. This is mainly due

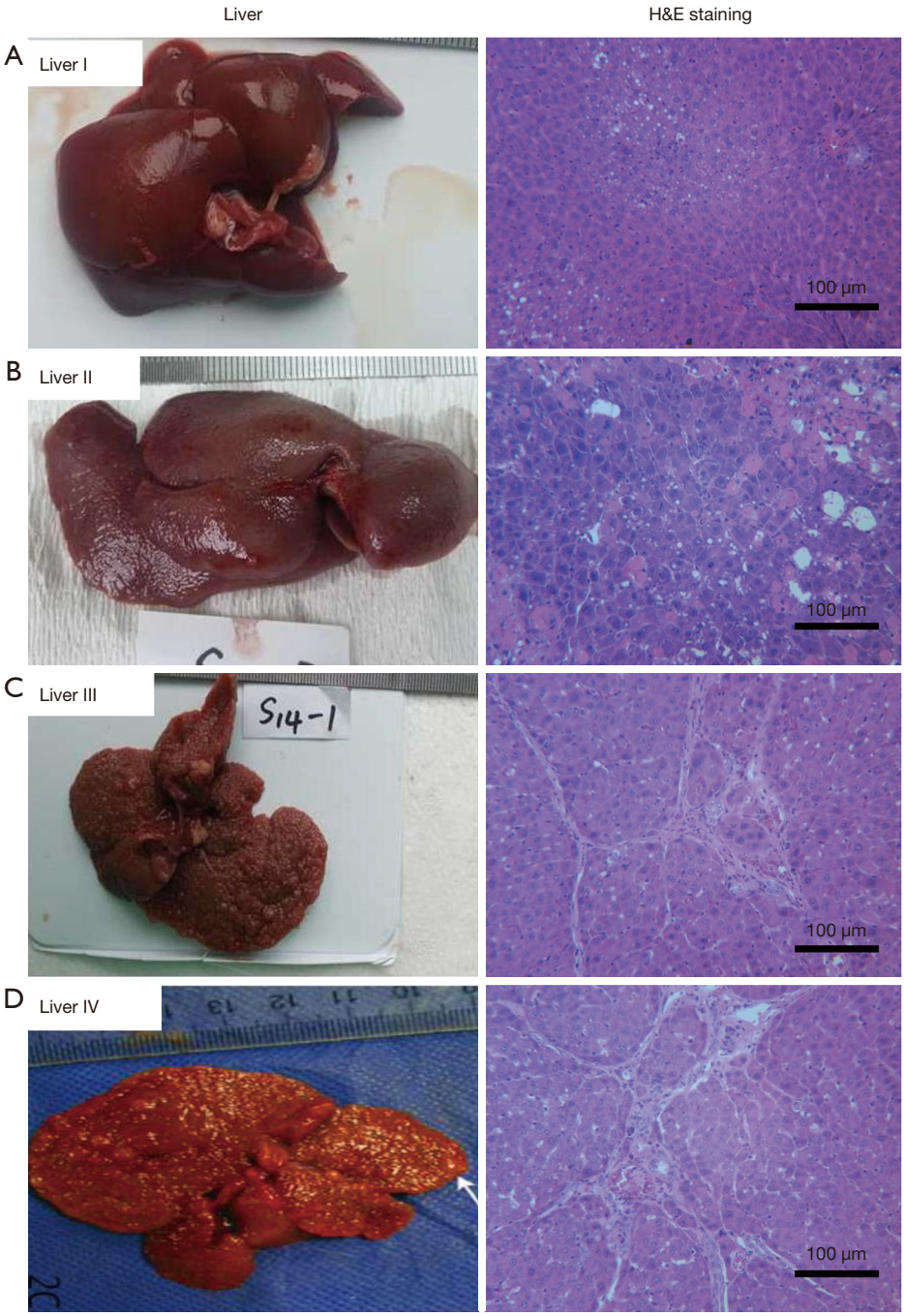

Figure 4 Pathological changes in the progression from hepatic fibrosis to cirrhosis. Liver tissues were examined using HE staining. (A) Level I, (B) Level II, (C) Level III, (D) Level IV. Magnification ×200.

to the fact that in the situation of liver fibrosis and liver cirrhosis, lipocytes, which are in the perisinusoidal space, are activated by cell factors and growth factors produced by hepatocytes, endotheliocytes, and inflammatory cells. These activated lipocytes are then transformed into myofibroblasts which synthesize abundant collagen. These collagenous fibers will surround the hepatic lobule central vein, portal area, and perisinusoidal space, which leads to

increasing pressure in the hepatica interstice. Furthermore, the diffusion of water molecules is limited, which decreases the value of the ADC (8). In contrast, an increasing ADC value leads to enlarging the discrete phase between water molecules (5), more flexible movement, and a significant reduction in signals. (9). Much research has indicated that when diffuse hepatocellular disease occur, abounding deposition of collagenous fibers in the intercellular space limits the diffusion of water molecules, which results in a lower ADC value than that of normal liver tissue (10). An increasing b value can partly inhibit the effect of blood microcirculation, thus, most research supports using a superior b value during DWI scanning. Kanematsu *et al.* (11) performed DWI scanning in 29 patients with liver cirrhosis and 29 normal volunteers, and b values were fixed at 0, 150, 250, 400, 600, and 800 s/mm^2. According to the results, the ADC value, which was used to diagnose and evaluate hepatic fibrosis, exhibited the highest accuracy when the b parameter was set at 400 s/mm^2. However, Fischer *et al.* (12) found that MR-DWI contributed to the early diagnosis of rat hepatic fibrosis, and the desirable b value should be 600 or 800 s/mm^2. In this study, when the b parameter was set at 600 s/mm^2, there was a better correlation between the pathological grade of liver fibrosis and the ADC value. Compared with the control group, the ADC parameter in different stages of liver fibrosis were obviously lower, which was similar with most previous research results (13,14).

The highest dependence was observed between the EADC value and the pathological grade of liver fibrosis with the b parameter fixed at 300 s/mm^2. This is mainly due to high quality EADC images, which result in a better ability to reflect the pathological changes in the liver without the influence of T_2 penetration (15). In the situation of setting the b value at 600 s/mm^2, the EADC value exhibited a limited correlation with the pathological grade of liver fibrosis, which was incongruous with most previous research (5,16). There are certain differences in the mechanisms of the progression from hepatic fibrosis to cirrhosis between rats and humans, particularly as the process was induced by TAA. Human cirrhosis is mainly caused by virus infection, yet chemical induction was performed in this research, which causes latent deposition of iron and glycogen in cells. Further changes in T_2WI sequence nodule signals were inconspicuous. The value of EADC was determined through the signal of DWI divided by the signal of T_2WI. With the development of cirrhotic nodules, the signal of DWI gradually declined, and no significant increases were found in the signal of T_2WI. Thus, there was no obvious change in the EADC value. Instead of $CC1_4$, TAA, which was more moderate, was used as an inducer in this research (17). At the early stage of hepatic fibrosis, TAA produced slight cellular inflammatory swelling and induced significant variation in microcirculation perfusion. The EADC value we examined was influenced by the situation of microcirculation perfusion. This value failed to veritably reflect the diffusion of extracellular water molecules in tissues in this situation. Meanwhile, with the increase of the b value, more sensitive magnetic susceptibility artifacts were generated with declining signal-noise ratio. When b>600 s/mm^2, DWI image noise in the liver was evidently enhanced, which could have influenced the accuracy of evaluating pathology and led to inexact measured effects in the EADC value (15). Moreover, the measured ADC and EADC values were more likely to be affected by susceptibility artifacts and microcirculation perfusion, which made it difficult to correctly quantify the extent of hepatic fibrosis (13). A further investigation on how to reduce the effect of microcirculation perfusion and the relevance between microcirculation perfusion and the values of ADC and EADC should be performed. At the same time, there have been some reports regarding the application of diffusion kurtosis imaging in liver-related diseases, which will be a hot topic in future research.

PCNA and Ki-67 are mature markers indicating cell proliferation, and in recent years they have been mainly utilized in various kinds of cancer research (4,5,8,12). High expression of PCNA reveals abundant synthesis of DNA in cells, which makes PCNA an excellent biomarker in the synthesis phase. As a PCNA, Ki-67 is expressed in the cell cycle except G0, and the most conspicuous expression can be observed in G2 and Lee *et al.* (13) investigated liver specimens of patients with cirrhosis or chronic hepatitis by PCNA. They found that PCNA could reveal the hepatocyte proliferation rate that was concerned with severity of hepatopathy in patients with chronic viral hepatitis, and PCNA was the strongest independent risk factor in hepatocarcinoma. There have also been some reports regarding the effect of PCNA in hepatoma and cancerous liver cirrhosis, and most research indicated that higher expression of PCNA can be found in hepatoma and cancerous liver cirrhosis compared to cirrhosis. As shown in the results, hepatocytes exhibited limited proliferation capacity in the situation of cirrhosis. Lee *et al.* (13) highlighted that there were few PCNA positive cells in the cirrhosis tissue, with diffusate distribution. Compared with that in cirrhosis tissue, positive expression of PCNA in

paraneoplastic hyperplastic nodules was evidently different, which are usually considered as precancerous lesions. In contrast, most cells in cirrhosis are in the stationary condition. These cells are a kind of highly mature cell which do not show any relationship with the occurrence of hepatoma. However, some reports (16,17) have indicated that the expression of PCNA was much higher in cirrhosis than in chronic hepatitis. There are few studies regarding the joint application of the 2 PCNAs in cirrhosis and hepatoma. Data in this study revealed that the PCNA and Ki-67 indexes in cirrhosis were significantly lower than in chronic hepatitis, which indicated that hepatocellular proliferation was more active in the situation of chronic hepatitis than in the state of cirrhosis. In the later stage of viral hepatitis, mature hepatocytes are widely infected by viruses, and these cells usually lose the capacity to proliferate. Furthermore, sustained death of hepatocytes demands continuous compensatory regeneration in the liver. Presently, proliferation of stem cells and oval cells were considered as the main sources of regenerative cells. Lee *et al.* (13) evaluated cirrhosis tissue by the liver fibrosis SSS score, and performed a correlation analysis with the results of PCNA. As shown in the results, hepatocellular proliferation in cirrhosis tissue had little relevance with the extent of fibrosis in the liver. The density of 46 samples of collagen fibers were examined in cirrhosis. According to the results, there was no correlation between the density of collagen fibers and the values of PCNA and Ki-67 in cirrhosis, which was similar with the abovementioned conclusions. As a reliable immunohistochemical marker that can assay cell proliferation, the anti-Ki-67 antibody can be used to detect the presence of proliferation-related nuclear antigens in order to recognize in which phase the cells are in. When cells are in G0, anti-Ki-67 staining is negative. In normal liver tissue, most cells are in the G0 phase. In contrast, cells exhibit reinforced proliferative activity in chronic hepatitis, cirrhosis, and hepatoma. The expression level of Ki-67 can evaluate the proliferation of cells, investigate tumor biological behaviors, and determine its risk (5). Ki-67 was used as a tumor marker to indirectly reflect the prognosis of a patient with hepatocarcinoma, and disease-free survival revealed a tight relationship with the growth speed of hepatoma (9,10). We found that the expression of Ki-67 was slightly positive in normal liver tissue, and the positive rate was 48.1% in hepatoma. In addition, the positive cell expression rate was obviously higher in vascular invasion than in no-vascular invasion, which indicated that Ki-67 was able to reveal the invasion, metastasis, and proliferation capacity of hepatocarcinoma, and could help predict recurrence and metastasis. When tumors were <5 cm, the level of Ki-67 was much less than that of tumors >5 cm, and the degree of differentiation in stage I-II was significantly lower than that of positive cell expression in stage III-IV. All these results prove that the lower the degree of differentiation, the higher the expression of Ki-67 and the proliferation of hepatocarcinoma. Ki-67 played an important role in the processes of hepatoma invasion and metastasis. Compared to the expression of Ki-67 in the extrahepatic bile duct and in cirrhosis, Ki-67 showed more active expression in hepatocarcinoma. The method to examine Ki-67, which was an effective index in judging the risk level of primary liver cancer, was easy and convenient, and can be utilized as an aided detection method to determine the risk level of partial cirrhosis.

Conclusions

In conclusion, the novel method, which combines immunohistochemical indexes with the values of ADC and EADC that were measured by the DWI method, can contribute to determining the pathological stage of hepatic fibrosis and cirrhosis, understanding the development of hepatopathy, predicting the pathological degree, and providing evidence for therapy. The application and accuracy of MRI still need to be improved by large sample and multiple parameter comparative analyses in further research.

Acknowledgments

Funding: This study was supported by Shanghai Municipal Commission of Health (12119b1400).

Footnote

Reporting Checklist: The authors have completed the ARRIVE reporting checklist. Available at https://dx.doi.org/10.21037/apm-21-1745

Data Sharing Statement: Available at https://dx.doi.org/10.21037/apm-21-1745

Conflicts of Interest: All authors have completed the ICMJE uniform disclosure form (available at https://dx.doi.org/10.21037/apm-21-1745). The authors have no conflicts

of interest to declare.

Ethical Statement: The authors are accountable for all aspects of the work in ensuring that questions related to the accuracy or integrity of any part of the work are appropriately investigated and resolved. This study was approved by the Ethics Committee of Dahua Hospital of Xuhui District, in compliance with Dahua Hospital of Xuhui District guidelines for the care and use of animals.

References

1. Lee SJ, Kim KH, Park KK. Mechanisms of fibrogenesis in liver cirrhosis: The molecular aspects of epithelial-mesenchymal transition. World J Hepatol 2014;6:207-16.
2. Sharma M, Rao PN, Sasikala M, et al. Autologous mobilized peripheral blood CD34(+) cell infusion in non-viral decompensated liver cirrhosis. World J Gastroenterol 2015;21:7264-71.
3. Gligorijević J, Djordjević B, Petrović A, et al. Expression of CD34 in cirrhotic liver--reliance to dedifferentiation. Vojnosanit Pregl 2010;67:459-62.
4. De Robertis R, D'Onofrio M, Demozzi E, et al. Noninvasive diagnosis of cirrhosis: a review of different imaging modalities. World J Gastroenterol 2014;20:7231-41.
5. Hua XP, Zhang L, Huang L, et al. Morphological differences of liver between two liver fibrosis models induced by dimethylnitrosamine and thioacetamide. Chin J Clin Pharmacol Ther 2014;19:747.
6. Tripathi DM, Vilaseca M, Lafoz E, et al. Simvastatin Prevents Progression of Acute on Chronic Liver Failure in Rats With Cirrhosis and Portal Hypertension. Gastroenterology 2018;155:1564-77.
7. Santiago-Rolón A, Purcell D, Rosado K, et al. A Comparison of Brunt's Criteria, the Non-Alcoholic Fatty Liver Disease Activity Score (NAS), and a Proposed NAS Scoring that Includes Fibrosis in Non-Alcoholic Fatty Liver Disease Staging. P R Health Sci J 2015;34:189-94.
8. Papalavrentios L, Sinakos E, Chourmouzi D, et al. Value of 3 Tesla diffusion-weighted magnetic resonance imaging for assessing liver fibrosis. Ann Gastroenterol 2015;28:118-23.
9. Liu Y, Meyer C, Xu C, et al. Animal models of chronic liver diseases. Am J Physiol Gastrointest Liver Physiol 2013;304:G449-68.
10. Xue G, Liu JF, Yan C, et al. Establishment of a rat model of thioacetamide. World Chinese Journal of Digestology 2015;23:1937-42.
11. Kanematsu M, Goshima S, Watanabe H, et al. Diffusion/perfusion MR imaging of the liver: practice, challenges, and future. Magn Reson Med Sci 2012;11:151-61.
12. Fischer MA, Donati OF, Reiner CS, et al. Feasibility of semiquantitative liver perfusion assessment by ferucarbotran bolus injection in double-contrast hepatic MRI. J Magn Reson Imaging 2012;36:168-76.
13. Lee JH, Park MJ, Kim JK, et al. Assessment of angiogenesis of hepatocellular carcinoma using dynamic contrast enhanced MR and histopathologic correlation in an experimental rat model. Hepatogastroenterology 2014;61:447-52.
14. Li G, Shen BX, Tan SP, et al. Feasibility Study of Assessing Liver Fibrosis with Volume Dynamic Contrast Enhanced MR Imaging of the Whole Liver. Chinese Journal of CT and MRI 2015;13:59-62.
15. Guan S, Zhao WD, Zhou KR, et al. Assessment of hemodynamics in precancerous lesion of hepatocellular carcinoma: evaluation with MR perfusion. World J Gastroenterol 2007;13:1182-6.
16. Elpek GÖ. Angiogenesis and liver fibrosis. World J Hepatol 2015;7:377-91.
17. Vanheule E, Geerts AM, Van Huysse J, et al. An intravital microscopic study of the hepatic microcirculation in cirrhotic mice models: relationship between fibrosis and angiogenesis. Int J Exp Pathol 2008;89:419-32.

(English Language Editor: C. Betlzar)

Cite this article as: Kong P, Yuan T, He Y, Wang S, Zhou X, Cao J. The correlation between magnetic resonance diffusion parameters and Ki-67 and PCNA in hepatic fibrosis and cirrhosis rats. Ann Palliat Med 2021;10(7):8112-8122. doi: 10.21037/apm-21-1745

